NASA Contractor Report 178197

ICASE REPORT NO. 86-68

ICASE

EFFICIENT SOLUTIONS OF TWO-DIMENSIONAL INCOMPRESSIBLE STEADY VISCOUS FLOWS

J. H. Morrison

M. Napolitano

Contract No. NAS1-18107

October 1986

INSTITUTE FOR COMPUTER APPLICATIONS IN SCIENCE AND ENGINEERING
NASA Langley Research Center, Hampton, Virginia 23665

Operated by the Universities Space Research Association

National Aeronautics and Space Administration

Langley Research Center
Hampton, Virginia 23665

EFFICIENT SOLUTIONS OF TWO-DIMENSIONAL INCOMPRESSIBLE STEADY VISCOUS FLOWS

J. H. Morrison
Analytical Services and Materials
Hampton, VA 23665

M. Napolitano
University of Bari, Italy and
Institute for Computer Applications in Science and Engineering

ABSTRACT

This paper provides a simple, efficient, and robust numerical technique for solving two-dimensional incompressible steady viscous flows at moderate-to-high Reynolds numbers. The proposed approach employs an incremental multigrid method and an extrapolation procedure based on minimum residual concepts to accelerate the convergence rate of a robust block-line-Gauss-Seidel solver for the vorticity-stream function Navier-Stokes equations.

Results are presented for the driven cavity flow problem using uniform and nonuniform grids and for the flow past a backward facing step in a channel. For this second problem, mesh refinement and Richardson extrapolation are used to obtain useful benchmark solutions in the full range of Reynolds numbers at which steady laminar flow is established.

The work of the second author has been supported by NASA Contract No. NAS1-18107 while he was in residence at ICASE, NASA Langley Research Center, Hampton, VA 23665 and by the Ministero della Pubblica Istruzione.

INTRODUCTION

This paper is concerned with the simulation of two-dimensional incompressible steady laminar separated flows at moderate-to-high Reynolds numbers (Re), using a simple, efficient, and robust numerical technique. Among the many numerical methods developed for the incompressible Navier-Stokes equations, those recently employed to solve high Re steady separated flows are very complex and sophisticated. For example, (i) Ghia et al. [1] use the cumbersome coupled strongly implicit method as a robust smoother for the already involved full-approximation-storage, full-multigrid method of Brandt [2], and (ii) Schreiber and Keller [3] solve a fourth order nonlinear problem for the stream function by a sequence of Newton and chord iterations, and use a costly L-U factorization with partial pivoting to solve the large sparse linear systems associated with the Newton iteration. In both techniques, the solution at a lower value of Re is to be used effectively to generate a sufficiently good initial condition. Therefore, it appears worthwhile to provide a numerical technique for solving high-Re separated flows, which is possibly as powerful and efficient as the best methods available to date but much simpler to implement and to use.

In the last few years, the second author has developed approximate factorization [4] and line relaxation [5] methods for solving the steady-state vorticity-stream function Navier-Stokes equations. These methods employ a two-level implicit Euler time stepping and the delta form [6] to discretize and linearize in time the unsteady governing equations and make effective use of a deferred correction strategy for the finite-difference spatial discretization; namely, second-order-accurate central differences are used for all spatial derivatives except the advection terms in the left hand side (LHS)

implicit operator, which are discretized using first-order-accurate upwind differences. In this way, an artifical viscosity is introduced which is proportional to a time derivative and thus vanishes as the sought steady-state solution is reached (see Appendix A). Also, the large 2x2 block-pentadiagonal matrix associated with the LHS implicit operator is diagonally dominant, so that the Alternating Direction Implicit (ADI) [4] or line Gauss-Seidel (LGS) [5] solution procedures enjoy the robustness and stability of upwind schemes and the accuracy of central-difference schemes. Both methods are very simple and have been reasonably successful in computing steady flows at moderate Reynolds numbers. However, their convergence rate invariably deteriorates when the computational mesh is refined and/or the Reynolds number is increased. In an attempt to overcome such a limitation, an incremental multigrid approach has been recently proposed [7], which is particularly suitable for this type of numerical methods, extremely simple, and does not require any additional storage with respect to the basic numerical scheme used as a smoother, nor any sophisticated strategy for cycling among the various grids. Therefore, it could be a viable alternative to more complicated multilevel methods. However, its validity has only been demonstrated for a model problem and is restricted to the case of uniform grids. It seems therefore necessary and appropriate to assess its merits and deficiencies versus more difficult problems and to further improve its performance, without affecting its major merit, namely, its simplicity.

These goals are achieved in this paper, which: (i) provides an improved version of the incremental multigrid method of [7], capable of handling meshes with reasonably high stretching; (ii) supplements such a method with an extrapolation technique based on minimum residual concepts [8] to further

enhance its efficiency; (iii) employs the resulting procedure to provide a benchmark solution for flow past a backward facing step in a channel in the full range of Re at which steady laminar flow is established.

NUMERICAL METHOD

The nondimensional vorticity-stream function Navier-Stokes equations are given in the standard Cartesian coordinate system, for simplicity, as

$$\omega_t + \psi_y \omega_x - \psi_x \omega_y - \frac{1}{Re} (\omega_{xx} + \omega_{yy}) = 0 \tag{1}$$

$$\psi_{xx} + \psi_{yy} + \omega = 0. \tag{2}$$

In Eqs. (1-2), Re is the Reynolds number, ω and ψ are the vorticity and the stream function, t is the time, x and y are the horizontal and vertical Cartesian coordinates, and subscripts indicate partial derivatives. Equations (1-2) are discretized in time by means of a two level implicit Euler time stepping and linearized using the delta approach [6], by neglecting terms of order Δ^2, to give:

$$\frac{\Delta\omega}{\Delta t} + \psi_y^n \Delta\omega_x + \omega_x^n \Delta\psi_y - \psi_x^n \Delta\omega_y - \omega_y^n \Delta\psi_x - \frac{1}{Re} (\Delta\omega_{xx} + \Delta\omega_{yy})$$

$$= - \psi_y^n \omega_x^n + \psi_x^n \omega_y^n + \frac{1}{Re} (\omega_{xx}^n + \omega_{yy}^n) \tag{3}$$

$$\Delta\psi_{xx} + \Delta\psi_{yy} + \Delta\omega = - \psi_{xx}^n - \psi_{yy}^n - \omega^n \tag{4}$$

where Δt is the time step, the superscript n indicates the known solution at the time level t^n and $\Delta\omega$, $\Delta\psi$ are the unknowns to be computed. Equations (3-4) are discretized in space using second-order-accurate central differences throughout, except for the advection derivatives $\Delta\omega_x$, $\Delta\psi_y$, $\Delta\omega_y$ and $\Delta\psi_x$ in the LHS of Eq. (3) which are discretized using first-order-accurate upwind differences according to the signs of ψ_y^n, ω_x^n, ψ_x^n, ω_y^n, and solved approximately by a block-ADI [4] or block-LGS method [5]. Only block-tridiagonal systems need to be solved along each row and column of the computational domain, and the double boundary condition for ψ can be easily imposed to provide the value of the vorticity at the wall directly (see Appendix B). Two points are of interest: (i) a relaxation-like time derivative needs to be added to the stream function equation if an ADI solution procedure is employed [9]; (ii) the advection terms in the right hand side of Eq. (4) are replaced by the corresponding conservative form

$$- (\psi_y \omega)_x + (\psi_x \omega)_y \tag{5}$$

which has been shown to provide more accurate results (see, e.g., [5]). This amounts again to employing a deferred correction approach, which is made particularly elegant and simple to implement by the use of the delta form [4]. Notice, in fact, that a standard central difference discretization of Eq. (5) requires values of ψ from the NW (North-West), SE (South-East), NE and SW gridpoints in the computational stencil and, if used in the implicit left hand side operator, would increase the number of nonzero diagonals in the resulting matrix and reduce its diagonal dominance. After every ADI or LGS

sweep, the solution is advanced as

$$(\psi, \omega)^n \leftarrow (\psi, \omega)^n + (\Delta\psi, \Delta\omega) \tag{6}$$

and the process is repeated until a satisfactory convergence criterion is met.

In order to describe the multigrid procedure employed in this study, Eqs. (3-4) are rewritten in a more general form, by dropping the superscript n and introducing superscripts H and h to indicate the current and the finest grids used in the computations (H = h, 2h, 4h, and 8h)

$$\frac{\Delta\omega^H}{\Delta t} + \psi_y^h \Delta\omega_x^H + \omega_x^h \Delta\psi_y^H - \psi_x^h \Delta\omega_y^H - \omega_y^h \Delta\psi_x^H - \frac{1}{Re}(\Delta\omega_{xx}^H + \Delta\omega_{yy}^H)$$

$$= C_h^H[-(\psi_y^h \omega^h)_x + (\psi_x^h \omega^h)_y + \frac{1}{Re}(\omega_{xx}^h + \omega_{yy}^h)] \tag{7}$$

$$\Delta\psi_{xx}^H + \Delta\psi_{yy}^H + \Delta\omega^H = C_h^H[-\psi_{xx}^h - \psi_{yy}^h - \omega^h] \tag{8}$$

where C_h^H indicates the standard 9-point collection operator, applied as many times as needed to go from the finest mesh h to the current mesh H. Starting from an arbitrary initial condition, Eqs. (7-8) are solved on the finest grid h -- where they coincide with Eqs. (3-4) -- by means of a two sweep alternating direction block-LGS iteration, to provide $\Delta\omega^h$, $\Delta\psi^h$; the solution ω^h, ψ^h is updated and Eqs. (7-8) are solved on successively coarser grids (H = 2h, 4h, and 8h); the entire process is repeated until the finest-grid residual is reduced to a suitably small value. In more detail, at every grid level H, the following steps are required by the proposed multigrid strategy: a) the coefficients in the LHS of Eqs. (7-8) are

evaluated at the H-mesh gridpoints using the finest-grid solution (ω^h, ψ^h) locally, whereas the RHS steady state residuals are evaluated on the finest grid h and collected up to the current grid H; b) Eqs. (7-8) are then solved approximately, using a single sweep of the aforementioned block-LGS smoother and homogeneous Dirichlet boundary conditions, to provide $\Delta\omega^H$, $\Delta\psi^H$; c) $\Delta\omega^h$, $\Delta\psi^h$ are evaluated as

$$(\Delta\omega^h, \Delta\psi^h) = I_H^h \, (\Delta\omega^H, \Delta\psi^H) \tag{9}$$

where I_H^h is the standard bilinear interpolation operator from the current grid H to the finest grid h; d) the finest-grid solution is updated as

$$(\omega^h, \psi^h) \leftarrow (\omega^h, \psi^h) + (\Delta\omega^h, \Delta\psi^h); \tag{10}$$

e) the vorticity at the boundaries is finally corrected so as to satisfy the no-slip boundary condition on the finest mesh (see Appendix B). All of the aforementioned steps are performed twice, with the block-LGS solution method marching from left to right and from top to bottom of the computational domain, respectively. A multigrid cycle is shown schematically in Figure 1, where it is seen to differ from both the more usual V and saw-tooth cycles. It is noteworthy that the proposed methodology is very simple, since it does not require any logical choices to be made and employs a single free parameter, namely, the time step Δt. Furthermore, it does not need any additional storage with respect to the basic smoother, insofar as only the finest-grid solution is computed and a single array is used for the deltas at all grid levels. However, its work per iteration is slightly greater than

that required by most current multigrid methods, due to the additional interpolations and collections needed to visit and update the finest-grid solution after every coarse-grid calculation and, due to its extreme simplicity, it is likely to be less efficient than more sophisticated multigrid methods.

The present approach, as described above, can be applied without any modifications to the vorticity-stream function equations written in a general curvilinear coordinate system ξ, η. The scale factors and the Jacobian of the transformation $(x, y) \rightarrow (\xi, \eta)$ are evaluated once and for all on the finest mesh and treated as the other variable coefficients in the linearized discrete equations arising at every grid level. However, numerical experiments performed for the case of the driven cavity flow problem have shown that the efficiency of the method rapidly deteriorates as the computational grid in the physical plane becomes increasingly nonuniform. Therefore, following the lead of several other workers (see, e.g., [10]), the 9-point collection operator for the residual has been modified so as to use weighed areas in physical space, and the bilinear interpolation operator has been modified so as to use distances among gridpoints also in physical space. More precisely, in order to collect a quantity f from the finest mesh h to the mesh $H = 2h$ at point P, the standard 9-point collection operator is given as:

$$C_h^{2h} f = \frac{1}{16} \{4f_{i,j} + 2f_{i-1,j} + 2f_{i,j+1} + 2f_{i+1,j} + 2f_{i,j-1} + \\ + f_{i-1,j-1} + f_{i-1,j+1} + f_{i+1,j+1} + f_{i+1,j-1}\} \tag{11}$$

whereas the modified collection operator is

$$C_h^{2h} f = \frac{1}{(A_1 + A_2 + A_3 + A_4)} \Big\{ A_1 (f_{i,j} + f_{i-1,j} + f_{i,j-1} + f_{i-1,j-1}) +$$

$$A_2 (f_{i,j} + f_{i+1,i} + f_{i,j-1} + f_{i+1,j-1}) + A_3 (f_{i,j} + f_{i-1,j} + f_{i,j+1} + f_{i-1,j+1})$$

$$+ A_4 (f_{i,j} + f_{i+1,j} + f_{i,j+1} + f_{i+1,j+1}) \Big\} \qquad (12)$$

where A_1, A_2, A_3 and A_4 are the areas of the four cells surrounding the gridpoint P (see Figure 2 which shows the 9-point computational stencil in the physical (x, y) and computational (ξ, η) planes). On the other hand, in order to interpolate a quantity f at point Q using the $f_{i,j}$ and $f_{i+2,j}$ values available on the coarser mesh, the standard bilinear interpolation operator is given as

$$I_{2h}^h f = \frac{f_{i+2,j} + f_{i,j}}{2} \qquad (13)$$

whereas the modified interpolation operator is

$$I_{2h}^h f = \frac{f_{i+2,j}(x_{i+1} - x_i) + f_{i,j}(x_{i+2} - x_{i+1})}{x_{i+2} - x_i} . \qquad (14)$$

Finally, in order to further enhance the convergence rate of the method, the following extrapolation technique based on minimum residual concepts [8] is used, after every k multigrid cycles, to obtain a new initial condition for the finest-mesh solution. Let f^{n-2}, f^{n-1}, f^n be the solution vectors (the vectors of all ω and ψ gridpoint values) at the end of the last

three cycles and R^{n-2}, R^{n-1}, R^{n} the corresponding residuals. A new initial solution f^{*} is obtained as

$$f^{*} = f^{n-1} + \zeta_1(f^{n} - f^{n-1}) + \zeta_2(f^{n-1} - f^{n-2}) \tag{15}$$

with ζ_1 and ζ_2 evaluated as follows. The residual R^{*} is assumed to depend linearly on ζ_1 and ζ_2, as

$$R^{*} = R^{n-1} + \zeta_1(R^{n} - R^{n-1}) + \zeta_2(R^{n-1} - R^{n-2}) \tag{16}$$

and the dot product $R^{*} \cdot R^{*}$ is minimized with respect to ζ_1 and ζ_2 to give:

$$\begin{pmatrix} a & b \\ b & c \end{pmatrix} \begin{pmatrix} \zeta_1 \\ \zeta_2 \end{pmatrix} = -\begin{pmatrix} d \\ e \end{pmatrix} \tag{17}$$

where

$$a = (R^{n} - R^{n-1}) \cdot (R^{n} - R^{n-1}) \tag{18}$$

$$b = (R^{n-1} - R^{n-2}) \cdot (R^{n} - R^{n-1}) \tag{19}$$

$$c = (R^{n-1} - R^{n-2}) \cdot (R^{n-1} - R^{n-2}) \tag{20}$$

$$d = R^{n-1} \cdot (R^{n} - R^{n-1}) \tag{21}$$

$$e = R^{n-1} \cdot (R^{n-1} - R^{n-2}). \tag{22}$$

It is noteworthy that such a procedure, which can be implemented using an arbitrary number of extrapolation parameters ζ_i [8], is extremely simple and employs a negligible amount of CPU time with respect to the basic solver. On the other hand, it requires additional memory, insofar as both the solution and the residual vectors are needed at previous iteration levels, and introduces an additional parameter in the proposed numerical method, namely, the interval of application of the extrapolation procedure, k. However, memory is not a problem, especially for the present case of two-dimensional flows and the convergence rate of the method has been found here to be rather insensitive to the value of k (see also [8]). A final remark is needed. In the present study, both the two-parameter extrapolation described above and the simpler one based on a single parameter ζ_1 have been employed. The two-parameter technique has consistently provided better results, but the efficiency gain achieved with respect to the simpler one-parameter approach has been rather limited, so that no attempt at using three or more parameters was made.

RESULTS

The numerical technique, as described in the previous section, has been applied to solve two viscous flow problems for several values of Re. The computations were always started from rest and used a nonoptimized time step, usually equal to one.

Flow in a driven cavity

The classical driven cavity flow [11] was considered at first in order to assess the performance: (i) of the basic multigrid method for increasing values of Re, without and with the extrapolation procedure; (ii) and of the modified method for increasingly nonuniform grids. As far as the first point is concerned, calculations were performed for Re = 1000 using a 129x129 uniform grid and from one to four grid levels, without and with the extrapolation technique applied every 20 iterations. The convergence histories are given in Figures 3 and 4, where the logarithm of the (L_1 norm of the) vorticity residual is plotted versus the work units, one work unit being the CPU time required to complete a two-sweep iteration on the finest mesh. In all cases, the residual has been dropped to machine zero on a Gould PN9005 computer using single precision arithmetic. It clearly appears that the multigrid method provides a considerable improvement over the basic smoother and that the extrapolation technique further enhances its efficiency. In order to assess the influence of the interval of application of the extrapolation procedure, k, on the convergence rate of the method, results have been obtained for various values of k and are given in Table 1, as the work units necessary for the vorticity residual to reach 10^{-4}. The value of k is seen to have a minor influence on the convergence rate of the method (see also [8]) and can thus be chosen somewhat arbitrarily.

k	10	15	20	25
work units	149	167	145	161

Table 1. Influence of k on the convergence rate of the method

The more difficult Re = 3200 flow case was then considered in order to further test the robustness of the method. Figure 5 provides the convergence histories of the basic smoother and of the four-grid multigrid method without and with the extrapolation procedure applied every 20 iterations. The basic smoother, although stable, is extremely slow to converge and also the multigrid method experiences rather severe difficulties before being able to reduce the residual effectively. Also, due to the lack of smoothness in the convergence history of the scheme, the extrapolation procedure is found to actually delay convergence. Incidentally, for Re = 10,000, convergence requires more than 10,000 work units, the extrapolation procedure again being beneficial. In conclusion, the present multigrid method is extremely robust but becomes inefficient for very high values of Re.

In order to address the second point of interest, namely, the performance of the improved method for the case of nonuniform grids, the same driven cavity problem was considered, again for Re = 1000 and 3200, by mapping the physical plane into a uniform-grid computational domain using the following analytical transformation [4], [5]:

$$\begin{pmatrix} x \\ y \end{pmatrix} = 0.5 + 0.5 \tanh\left[C\left(\begin{matrix} 2\xi \\ 2\eta \end{matrix} - 1\right)\right]/\tanh(C). \qquad (23)$$

For $C \ll 1$, the x and y lines are practically equally spaced, whereas, as C increases, more and more gridlines are concentrated near the boundaries of the unit-square physical domain. The governing equations in terms of the ξ and η variables are given in [5] and the scale factors and the Jacobian of the transformation (23) are computed numerically using second-order-accurate central differences everywhere except at the boundaries, where three-point one-sided differences are used [5]. In the present calculations a 65x65 uniform grid in the ξ, η computational plane was used, for several values of C, and a reduced value of the time step, $\Delta t = 0.2$, was always employed, as already in [5]. The improved four-grid multigrid method converged without any difficulty for C as high as 1.4, for which the maximum-to-minimum Δx (Δy) ratio is equal to 4.45. Also, the extrapolation procedure improved the efficiency of the method for both $Re = 1000$ and $Re = 3200$, convergence to machine zero requiring about 400 and 1000 work units, respectively. For completeness, the numerical results are given in Table 2 as the maximum values of the stream function (ψ_M) and the values of the vorticity at the center of the moving plate (ω_C). The corresponding results obtained using uniform grids of 97x97 and 129x129 gridpoints are also given for comparison. The 65x65 nonuniform-grid results are as accurate as the 129x129 uniform-grid ones, so that, for the present problem, the nonuniform-grid method results to be more effective overall. However, the present approach is considered to be inadequate to compute external flows requiring highly stretched grids.

			ψ_M	ω_C
	97x97	uniform	.1174	14.95
Re = 1000	129x129	uniform	.1180	14.88
	65x65	nonuniform	.1181	14.88
	97x97	uniform	.1166	26.98
Re = 3200	129x129	uniform	.1187	26.16
	65x65	nonuniform	.1193	25.96

Table 2. Driven cavity flow results

Flow past a backward facing step

The flow past a backward facing step in a channel, see Figure 6, is a very interesting problem which has been chosen by the organizers of a GAMM workshop as the test case for comparing a great number of codes for solving the incompressible Navier-Stokes equations. From the results presented at the workshop [12], it clearly appears that for $Re \geq 500$ most methods face convergence difficulties and/or need some kind of upwinding to handle the flow regions where convection dominates diffusion. Physically, as clearly shown by the very careful experiments of Armaly et al. [13], the structure of the flow becomes more and more complicated as Re increases: the flow, which always separates over the step, reattaches downstream at a distance which increases

with Re and, for sufficiently high values of Re, a secondary separation region develops on the wall opposite to the step. This problem was thus chosen as a severe test for the present approach using central differences for the RHS steady state residual. The computational domain is limited to the interior of the channel immediately at the right of the step and a fully developed (Couette flow) parabolic velocity profile is used as a boundary condition in the upper half of the left boundary (h/H = 0.5, see Figure 6) [13, 14]. The proposed approach, without and with the extrapolation technique has been employed using uniform grids with 49x49, 65x49, 81x49 and 97x49 gridpoints for the cases Re = 200, 400, 600 and 800, respectively, the downstream boundary condition being set at a distance from the step equal to 7.5, 10, 12.5 and 15. The nondimensional height of the channel H is equal to 1 and the maximum value of the nondimensional longitudinal velocity component at inlet is equal to 1.5 [14]. At the outlet of the channel, second-order-accurate three-point homogeneous Neumann boundary conditions are used for both ψ and ω, to minimize the upstream influence due to imposing an asymptotic condition at a finite downstream distance. At the inlet and at all of the walls, standard no-slip conditions are prescribed, as shown in Appendix B. In particular, at the inlet, ψ_{yy}, which is discontinuous at the corner C, is evaluated analytically, with the gridpoint C obviously being considered part of the inlet-flow domain ($\psi_{yy} = 12$). In all cases, no convergence difficulty was encountered, again starting all computations from rest and always using $\Delta t = 1$. The convergence histories for the method, using from 1 to 4 grid levels, without and with the extrapolation applied every 20 iterations, are given in Figures 7 and 8 for Re = 200, and in Figures 9 and 10 for Re = 800. For the simpler Re = 200 flow case, using a

rather coarse 49x49 finest mesh, the multigrid approach reaches its peak efficiency when using 3 grid levels, without the extrapolation, and 2 grid levels, with the extrapolation. For the more difficult Re = 800 flow case, using a 97x49 finest-grid, the efficiency of the multigrid method always improves with increasing number of grid levels. In all cases, the extrapolation significantly improves the performance of the approach.

An efficient and second-order-accurate method being available, solutions were obtained for all four cases doubling the number of mesh intervals in both directions, so as to provide a benchmark solution for this very interesting problem. Figures 11 and 12 show the lower and upper walls vorticity distributions obtained using 97x97, 129x97, 161x97 and 193x97 gridpoints for Re = 200, 400, 600 and 800, respectively. On the same figures, the results obtained using the coarser grids are also given as symbols. It appears that for Re = 200 and 400 grid convergence has been achieved, whereas for Re = 600 and 800 further mesh refinement is probably warranted. However, the two different grid results in Figures 11 and 12 are reasonably close, so that Richardson extrapolation can be used with confidence to obtain a benchmark solution: Table 3 provides the values of the locations of the reattachment point for the primary separation bubble (X1R) and of the separation and reattachment of the secondary separation bubble (X2S, X2R), divided by the height of the step h [14], obtained using linear interpolation between the two gridpoints at which the wall vorticity changes sign and Richardson extrapolation to zero step size. Incidentally, the numerical results used for the extrapolation are converged to machine zero, using double precision arithmetic.

Re	200	400	600	800
X1R/h	5.34	8.63	10.72	12.16
X2S/h	-	7.96	8.71	9.67
X2R/h	-	10.44	16.23	20.96

Table 3. Benchmark Results

It needs to be remarked that, for all values of Re, the far downstream values of the vorticity on the lower and upper walls should be 3 and -3, respectively. From the results of Figures 11 and 12, one may thus believe that the outflow boundary conditions have not been imposed far enough downstream, especially for the higher values of Re. Therefore, the coarser grid computations were repeated for the cases Re = 200 and Re = 800, moving the outflow boundary-condition locations to x = 15 and x = 25, respectively, and increasing the number of longitudinal gridpoints to maintain the same value of Δx. The results for the lower and upper walls vorticity are given in Figures 13 and 14 for both sets of calculations. The vorticity is seen to tend to its asymptotic value correctly and the results obtained using the two different locations for the outflow boundary conditions are in perfect agreement. The usefulness of using outflow conditions of Neumann type is thus clearly demonstrated so as the validity of the results in Table 3 as a benchmark solution.

CONCLUSIONS

A simple, robust, and efficient method has been developed for solving two-dimensional steady viscous flows. An incremental alternating direction, block-line-Gauss-Seidel relaxation method using first-order-accurate upwind differences in the left hand side implicit operator and second-order-accurate central differences in the right-hand-side steady-state residual is used as smoother within a very simple multigrid algorithm, supplemented by an extrapolation procedure based on minimum residual concepts. The proposed technique has been tested versus the classical driven cavity flow, for values of the Reynolds number (Re) as high as 10,000, and used to provide useful benchmark solutions for flow past a backward facing step in a channel, for values of Re covering the full range at which steady laminar flow exists. The convergence rate of the method, which always starts from an arbitrary initial condition and marches towards steady state using a simple multigrid cycle without any optimization, logical choices or adjustable parameters, is very satisfactory for moderate-to-high values of Re. However, a more sophisticated approach is required for very high values of Re and/or highly nonuniform grids.

ACKNOWLEDGMENTS

The work of the first authour has been supported by NASA training grant NGT 47-004-808 while he was a graduate student at Virginia Polytechnic Institute and State University. His advisor, Professor B. Grossman, has provided continuous encouragement and support.

REFERENCES

[1] U. Ghia, K. N. Ghia, and C. T. Shin, "High-Re solutions for incompressible flow using the Navier-Stokes equations and a multigrid method," J. Comp. Physics, Vol. 48, 1982, pp. 387-411.

[2] A. Brandt, "Multi-level adaptive solutions to boundary-value problems," Math. of Comp., Vol. 31, No. 138, 1977, pp. 333-390.

[3] R. Schreiber and H. B. Keller, "Driven cavity flows by efficient numerical techniques," J. Comp. Physics, Vol. 49, 1983, pp. 310-333.

[4] M. Napolitano, "Efficient ADI and spline ADI methods for the steady-state Navier-Stokes equations," Int. J. Num. Methods in Fluids, Vol. 4, 1984, pp. 1101-1115.

[5] M. Napolitano and R. W. Walters, "An incremental block-line-Gauss-Seidel method for the Navier-Stokes equations," AIAA Journal, Vol. 24, May 1986, pp. 770-776.

[6] R. M. Beam and R. F. Warming, "An implicit factored scheme for the compressible Navier-Stokes equations," AIAA Journal, Vol. 16, April 1978, pp. 393-402.

[7] M. Napolitano, "An incremental multigrid strategy for the fluid dynamic equations," AIAA Paper No. 85-1517, 1985.

[8] M. Hafez, E. Parlette, and M. Salas, "Convergence acceleration of iterative solutions of Euler equations for transonic flow computations," AIAA Paper No. 85-1641, 1985.

[9] R. T. Davis, "Numerical solutions of the Navier-Stokes equations for symmetric laminar incompressible flow past a parabola," J. Fluid Mechanics, Vol. 51, Pt. 3, 1972, pp. 417-433.

[10] W. J. Usab, Jr., "Embedded mesh solutions of the Euler equations using a multiple-grid method," Ph.D. Thesis, M.I.T., Cambridge, MA, December 1983.

[11] O. R. Burggraf, "Analytical and numerical studies of the structure of steady separated flows," J. Fluid Mechanics, Vol. 24, Pt. 1, 1966, pp. 113-151.

[12] K. Morgan, J. Periaux, and F. Thomasset (Eds.), "Analysis of laminar flow over a backward facing step," Notes on Numerical Fluid Mechanics, Vol. 9, Vieweg, 1984.

[13] B. F. Armaly, F. Durst, J. C. F. Pereira, and B. Schonung, "Experimental and theoretical investigation of backward-facing step flow," J. Fluid Mech., Vol. 127, 1983, pp. 473-496.

[14] J. Kim and P. Moin, "Application of a fractional-step method to incompressible Navier-Stokes equations," J. Comp. Physics, Vol. 59, No. 2, June 1985, pp. 308-323.

[15] P. K. Khosla and S. G. Rubin, "A diagonally dominant second-order-accurate implicit scheme," Computers and Fluids, Vol. 2, 1974, pp. 207-209.

APPENDIX A

Consider the linear advection diffusion equation

$$u_t + cu_x - \varepsilon u_{xx} = 0 \tag{A1}$$

where c is a function of x and can be either positive or negative. The discrete form of Eq. (A1) using the delta approach and a deferred correction strategy as done in this paper for the vorticity-stream function equations is

$$\frac{\Delta u_i}{\Delta t} + \frac{c_i + |c_i|}{2} \frac{\Delta u_i - \Delta u_{i-1}}{\Delta x} + \frac{c_i - |c_i|}{2} \frac{\Delta u_{i+1} - \Delta u_i}{\Delta x} \tag{A2}$$

$$- \varepsilon \frac{\Delta u_{i+1} - 2\Delta u_i + \Delta u_{i-1}}{\Delta x^2} = -c_i \frac{u_{i+1} - u_{i-1}}{2\Delta x} + \frac{\varepsilon\, u_{i+1} - 2u_{i+1}\, u_{i-1}}{\Delta x^2}$$

The two incremental advection terms in Eq. (A2) can be written as

$$c_i \frac{\Delta u_{i+1} - \Delta u_{i-1}}{2\Delta x} - \frac{|c_i|\ \Delta x}{2} \frac{\Delta u_{i-1} - 2\Delta u_i + \Delta u_{i+1}}{\Delta x^2} \tag{A3}$$

so that Eq. (A2) is easily seen to be an implicit central-in-space finite difference discretization of Eq. (A1), plus an artificial viscosity term which is the backward-in-time central-in-space finite difference approximation of

$$\frac{-|c_i|\ \Delta x\ \Delta t}{2} u_{xxt} \tag{A4}$$

and thus vanishes identically at steady state. Similarly, it is seen that the four advective terms in the LHS of Eq. (3) are equivalent to the corresponding central difference approximations plus artificial viscosity terms which vanish at steady state. It is to be pointed out that the discretization used in Eq. (A2) is the delta form of the one proposed by Khosla and Rubin [16] and is easily seen to provide a diagonally dominant matrix for the LHS implicit operator.

APPENDIX B

Let us consider the gridpoints adjacent to the boundary line BB, together with a mirror image point, 0, outside the computational domain [11] as shown in Figure 15. At gridpoint 1, the double specification for the stream function is given as:

$$\psi_1 = a \tag{B1}$$

$$(\psi_x)_1 = b. \tag{B2}$$

Equation (B2) is discretized using a third-order-accurate four point difference

$$\frac{(-\psi_3 + 6\psi_2 - 3\psi_1 - 2\psi_0)}{6\,\Delta x} = b. \tag{B3}$$

In order to eliminate the additional unknown ψ_0, the steady state stream funtion equation is also used at the boundary gridpoint 1 [11]

$$\psi_{xx} + \psi_{yy} + \omega = 0 \tag{B4}$$

which is discretized as:

$$\frac{\psi_0 - 2\psi_1 + \psi_2}{\Delta x^2} + \psi_{yy} + \omega_1 = 0 \tag{B5}$$

where the ψ_{yy} term is left unchanged for convenience. By combining Eqs. (B3) and (B5), the following equation for the vorticity at the boundary, ω_1,

is obtained:

$$\omega_1 = -\psi_{yy} + \frac{6\ b\ \Delta x + 7\ \psi_1 - 8\ \psi_2 + \psi_3}{2\ \Delta x^2} \ . \qquad \text{(B6)}$$

Equations (B1) and (B6) are written in delta form and used, together with the internal-gridpoints discrete equations and the corresponding conditions for the RHS boundary, to provide a 2x2 block-tridiagonal system which is solved very efficiently by block-tridiagonal elimination. Notice that in Eq. (B6) ψ_{yy} is either zero, if line BB is a solid boundary, or is known, if line BB is a flow-inlet boundary. Also, from Eq. (B6), it clearly appears that a third order accurate discretization of Eq. (B2) is needed to obtain a second order accurate ω_1 (see also [1]). Finally, in the present multigrid method, Eq. (B6) and the corresponding ones are also used to correct the finest-grid solution at the boundaries, after every coarse-to-fine-grid interpolation.

FIGURE CAPTIONS

Figure 1. Schematic of the multigrid cycle.

Figure 2. Finite difference stencil in physical (x,y) and computational (ξ,η) planes.

Figure 3. Convergence histories of the multigrid method using 1, 2, 3 and 4 grid levels for Re = 1000.

Figure 4. Convergence histories of the multigrid method with extrapolation using 1, 2, 3 and 4 grid levels for Re = 1000.

Figure 5. Convergence histories of the basic solver and of the four-grid multigrid without and with extrapolation (dotted line) for Re = 3200.

Figure 6. Flow past a backward facing step in a channel: geometry and boundary conditions.

Figure 7. Convergence histories of the multigrid method using 1, 2, 3 and 4 grid levels for Re = 200.

Figure 8. Convergence histories of the multigrid method with extrapolation using 1, 2, 3 and 4 grid levels for Re = 200.

Figure 9. Convergence histories of the multigrid method using 1, 2, 3 and 4 grid levels for Re = 800.

Figure 10. Convergence histories of the multigrid method with extrapolation using 1, 2, 3 and 4 grid levels for Re = 800.

Figure 11. Effect of grid refinement on the lower wall vorticity for various values of Re.

Figure 12. Effect of grid refinement on the upper wall vorticity for various values of Re.

Figure 13. Effect of downstream boundary condition location on the lower wall vorticity for two values of Re.

Figure 14. Effect of downstream boundary condition location on the upper wall vorticity for two values of Re.

Figure 15. Computational gridpoints around a boundary line.

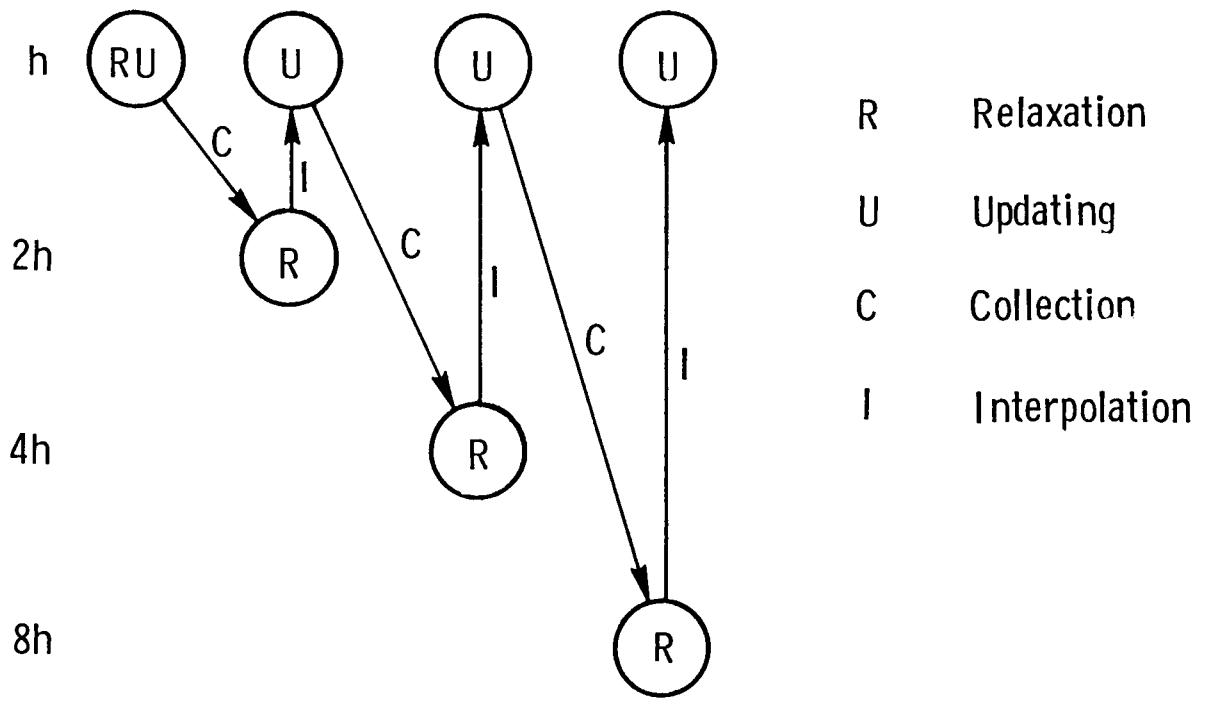
h
2h
4h
8h
RU
U
U
U
R
R
R
C
I
C
I
C
I
R Relaxation
U Updating
C Collection
I Interpolation

Figure 1

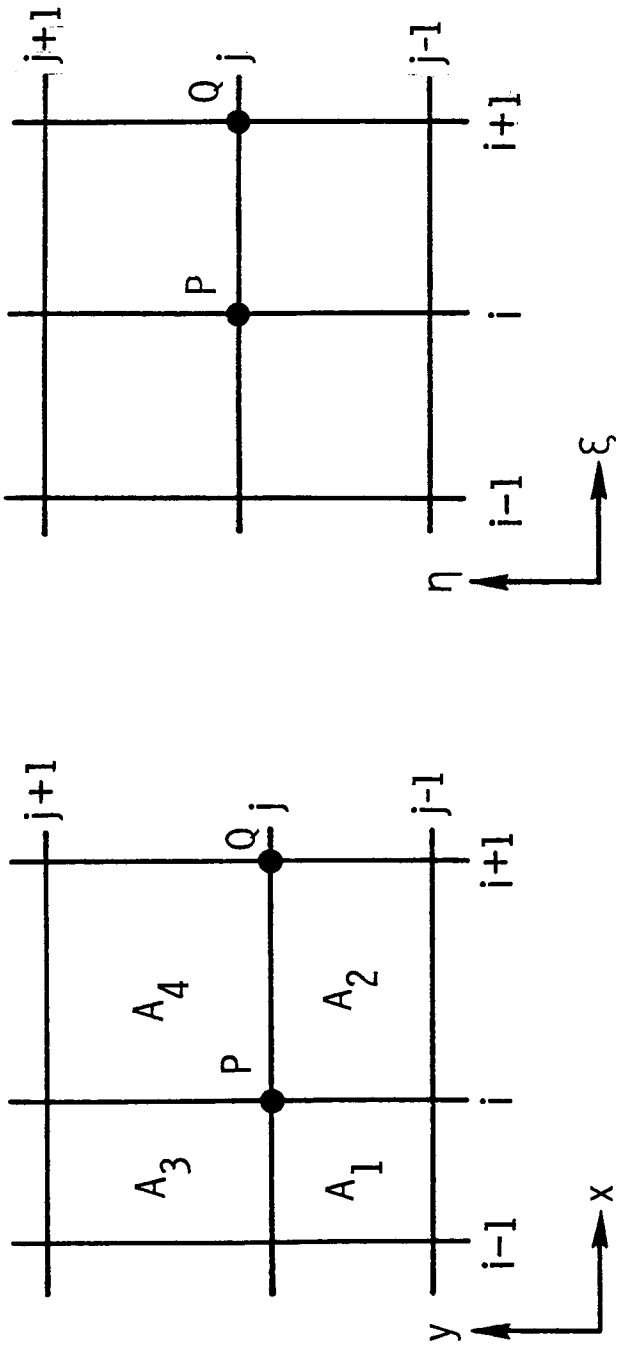

Figure 2

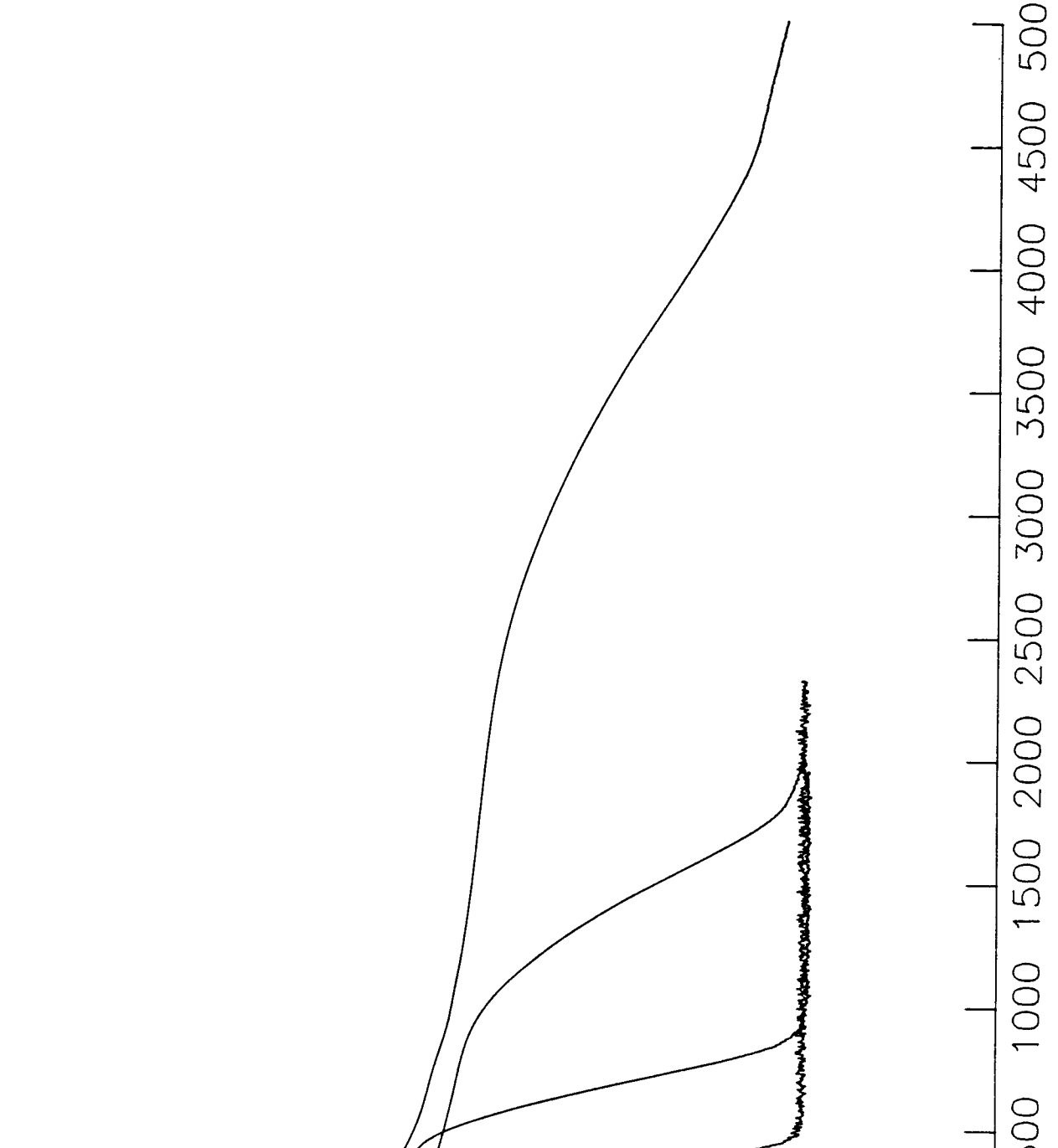
Log(Residual)
2
1
0
-1
-2
-3
-4
-5
-6
0
500
1000
1500
2000
2500
3000
3500
4000
4500
5000
Work Units

Figure 3

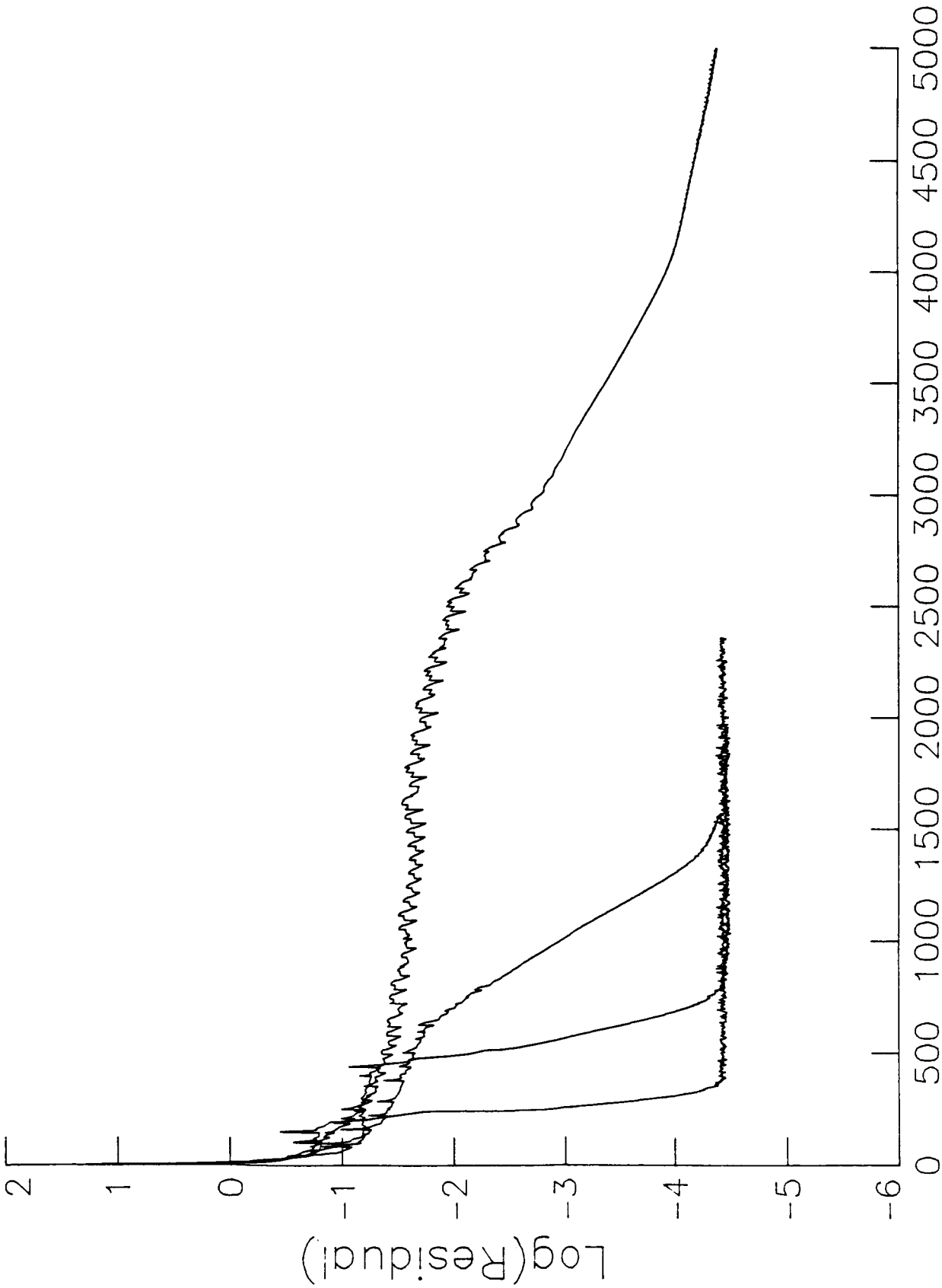
Log(Residual)
2
1
0
-1
-2
-3
-4
-5
-6
0
500
1000
1500
2000
2500
3000
3500
4000
4500
5000
Work Units

Figure 4

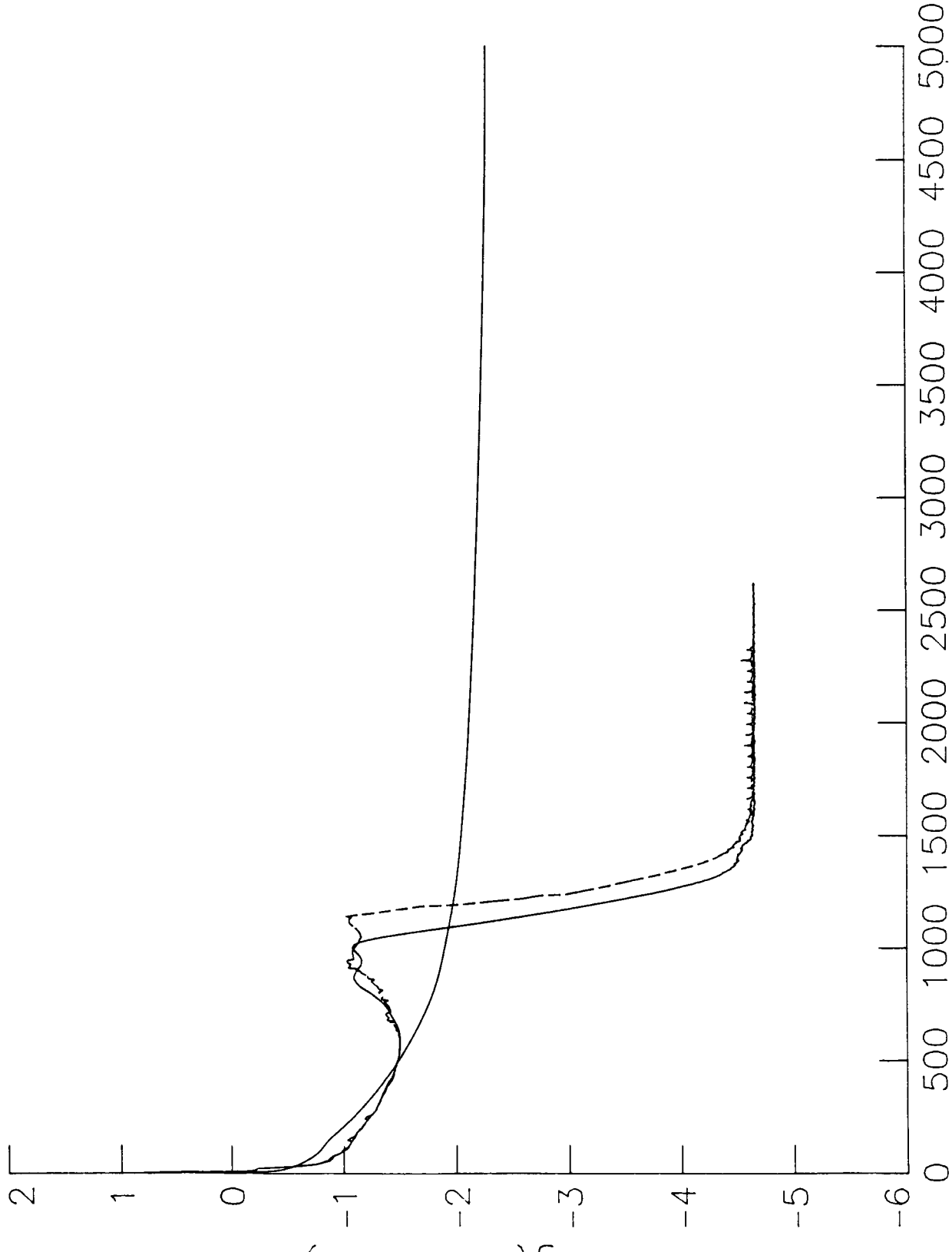
Log(Residual)
2
1
0
-1
-2
-3
-4
-5
-6
0
500
1000
1500
2000
2500
3000
3500
4000
4500
5000
Work Units

Figure 5

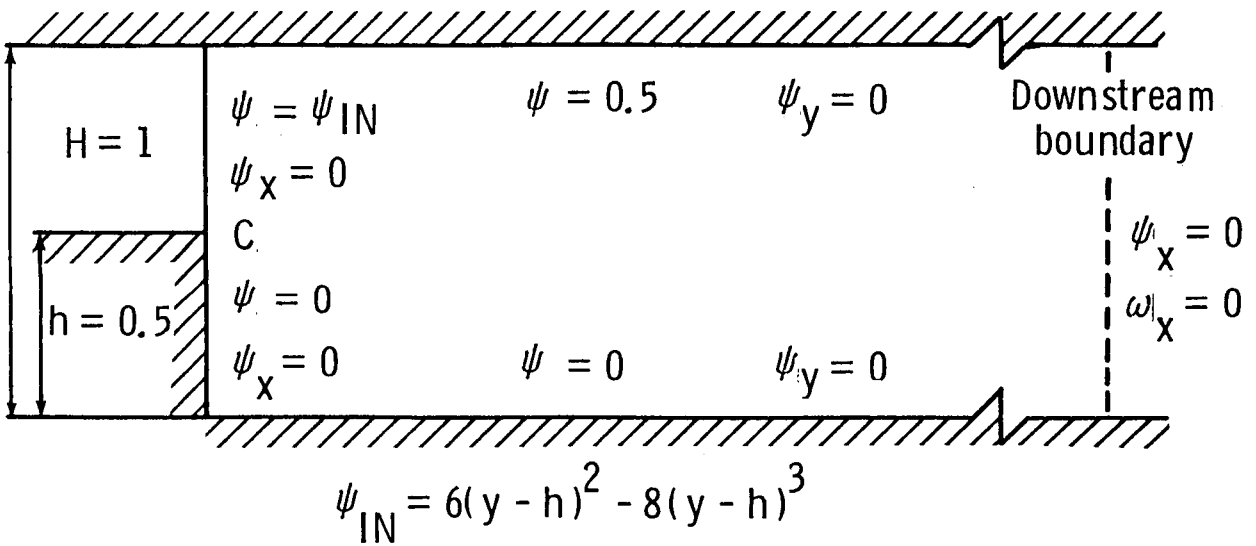
H = 1
h = 0.5
$\psi = \psi_{IN}$
$\psi_x = 0$
C
$\psi = 0$
$\psi_x = 0$
$\psi = 0.5$
$\psi = 0$
$\psi_y = 0$
$\psi_y = 0$
Downstream boundary
$\psi_x = 0$
$\omega_x = 0$
$\psi_{IN} = 6(y - h)^2 - 8(y - h)^3$

Figure 6

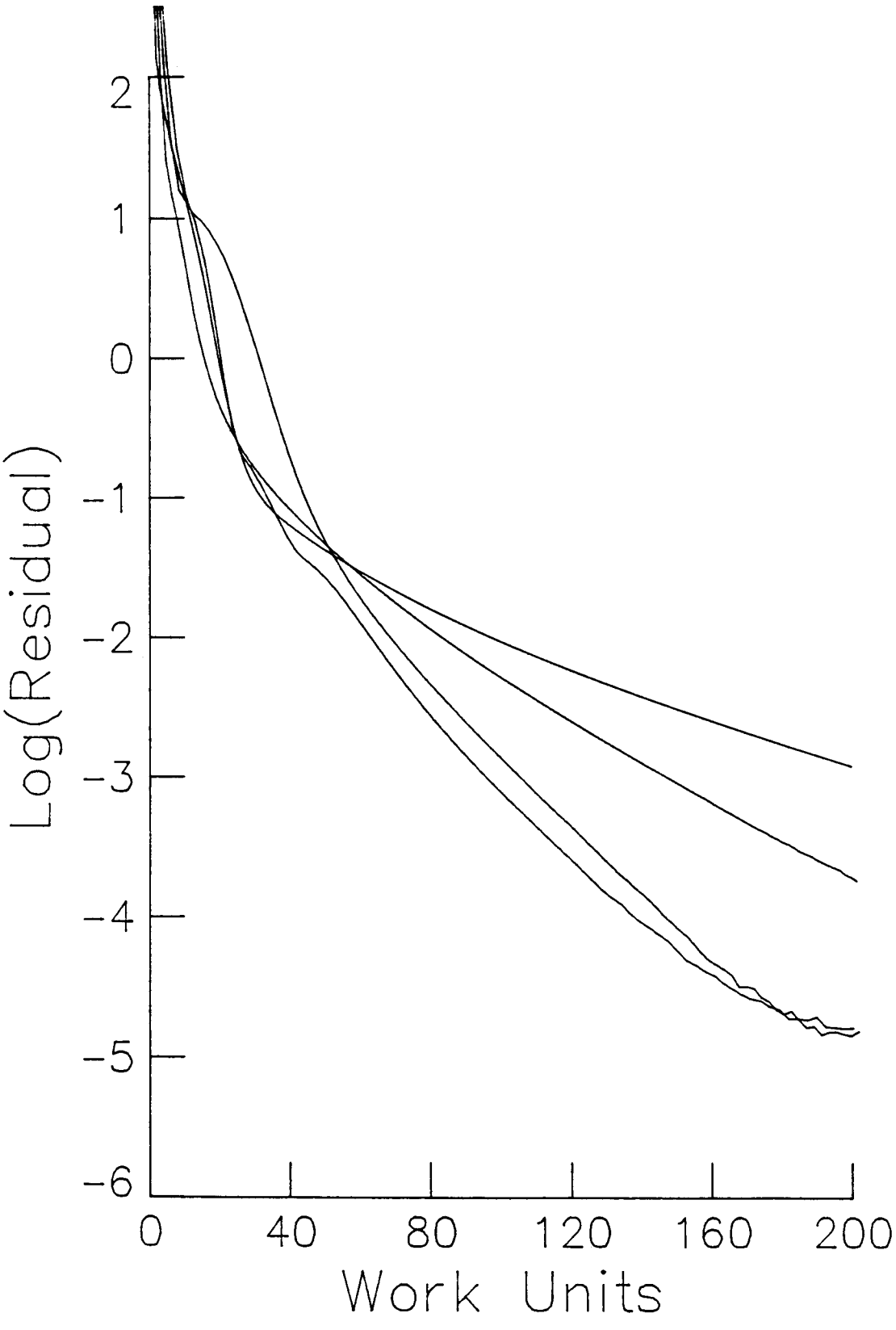

Figure 7

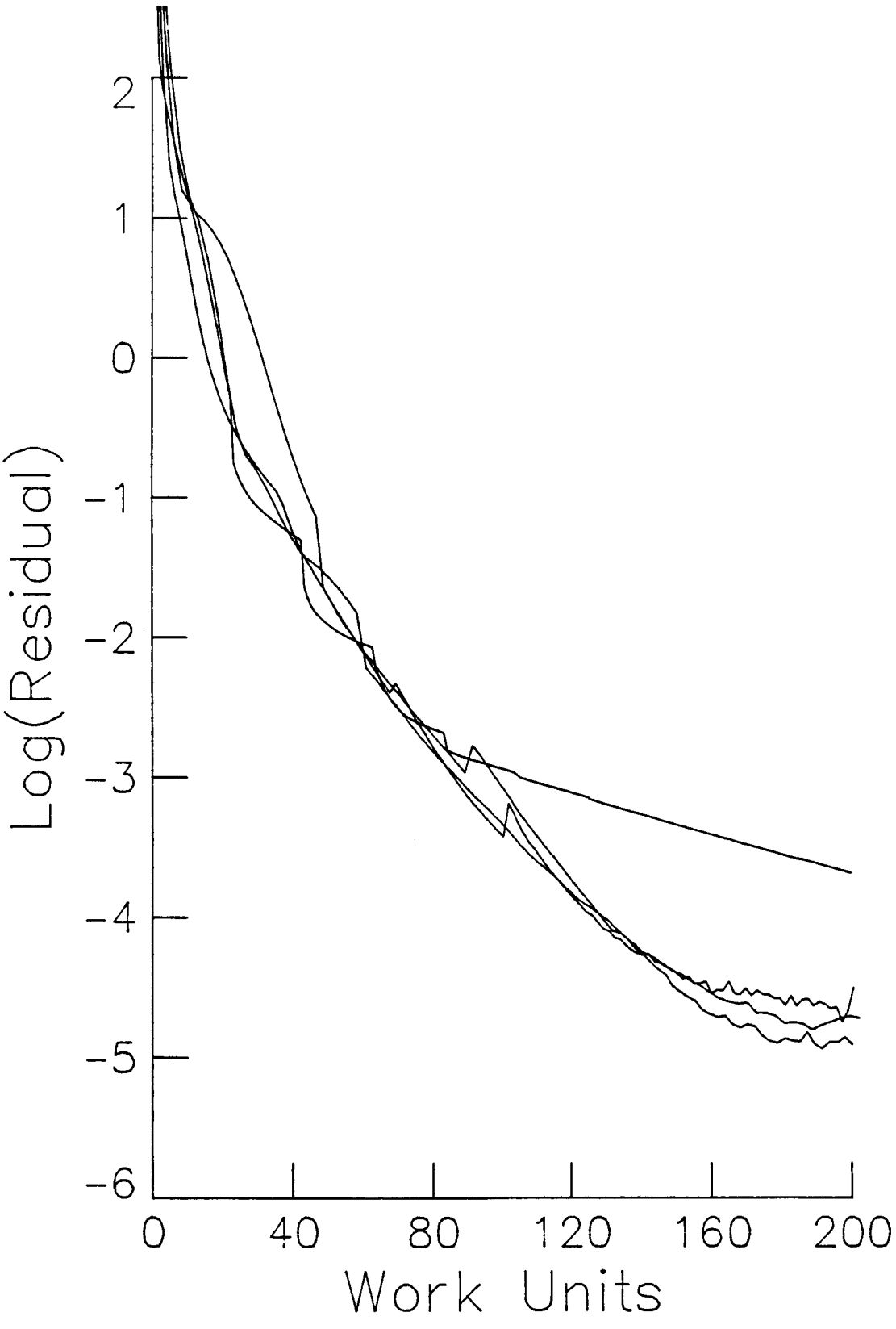

Figure 8

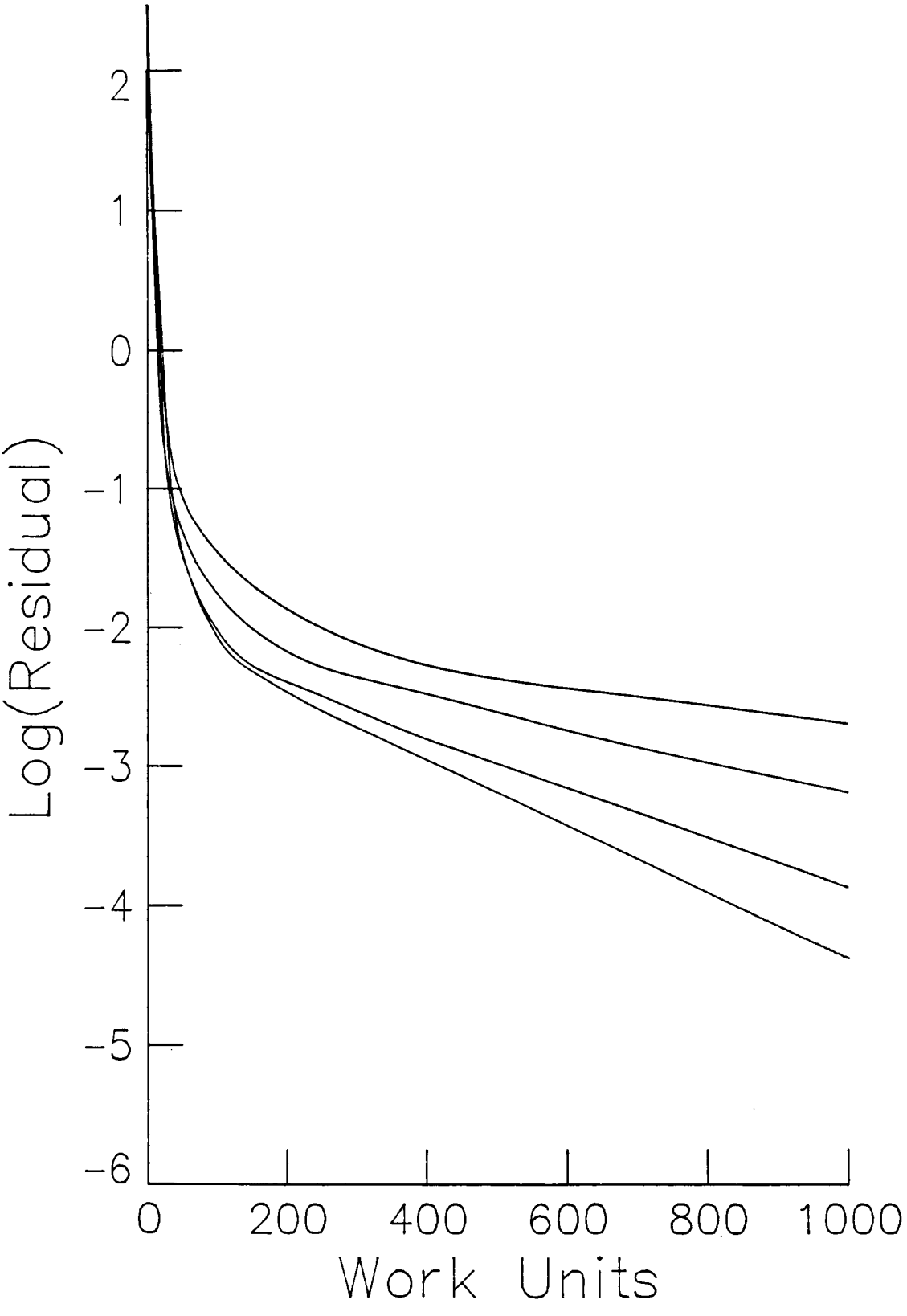

Figure 9

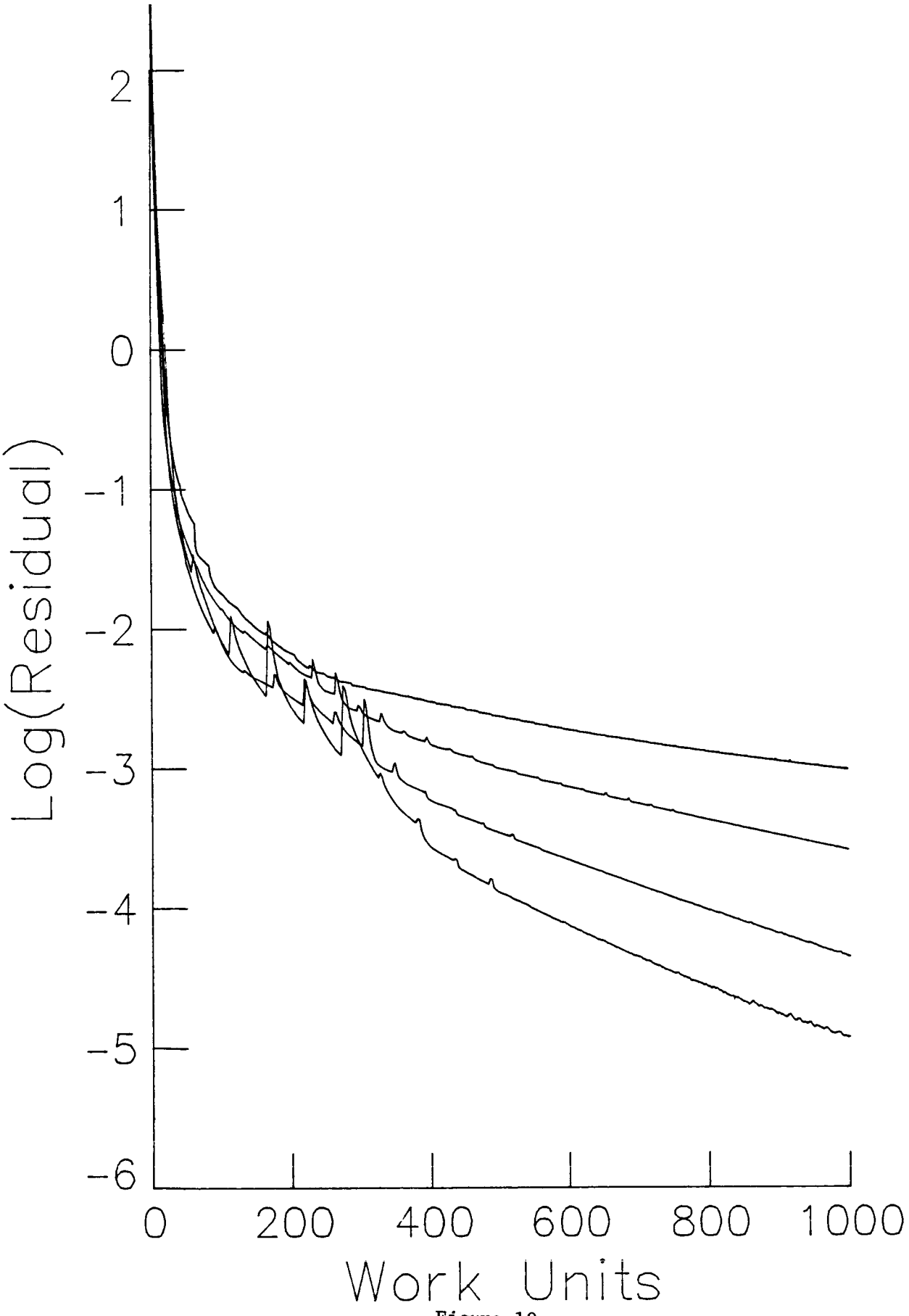

Figure 10

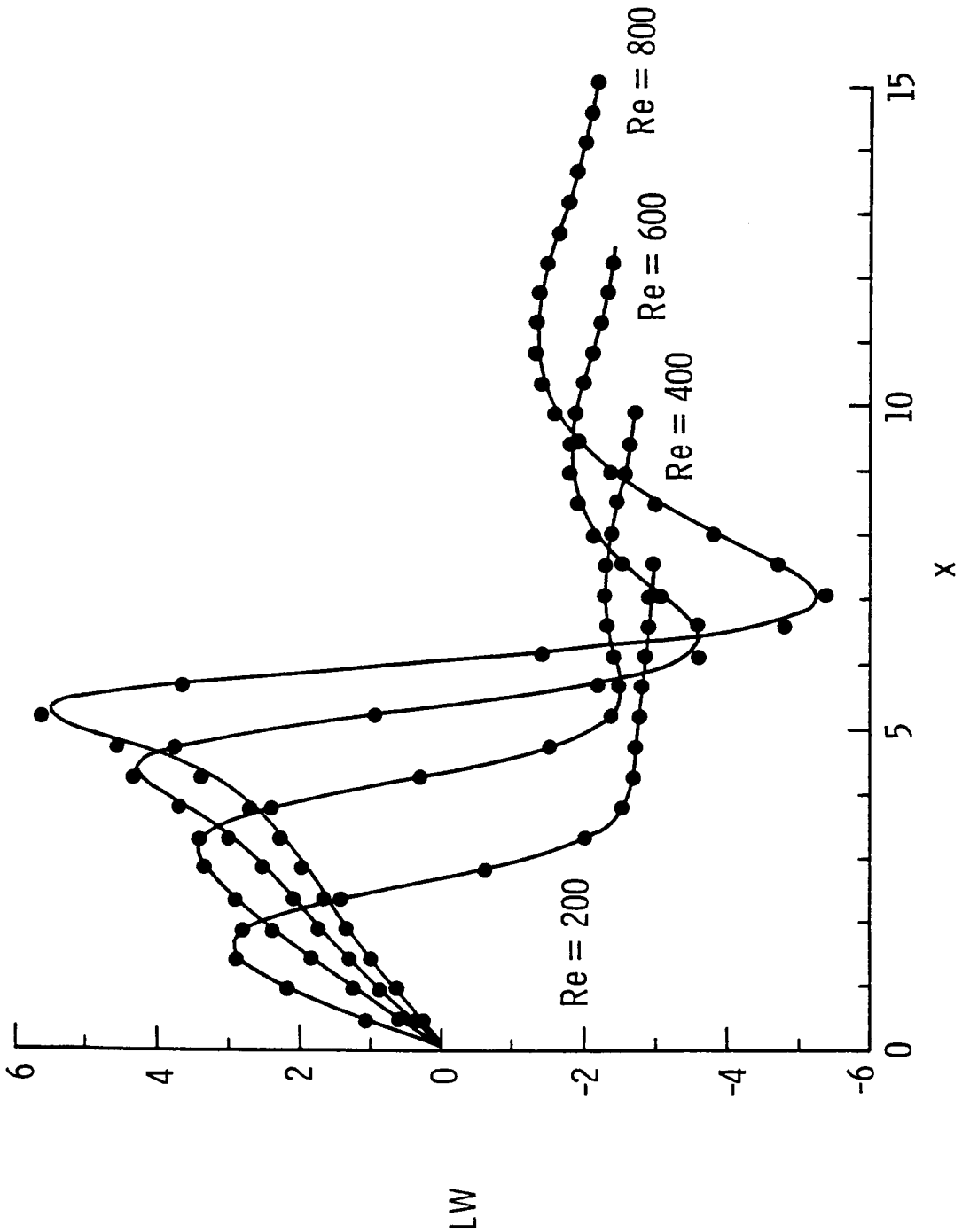
Re = 800
Re = 600
Re = 400
Re = 200
6
4
2
0
-2
-4
-6
0
5
10
15
x
ω_{LW}

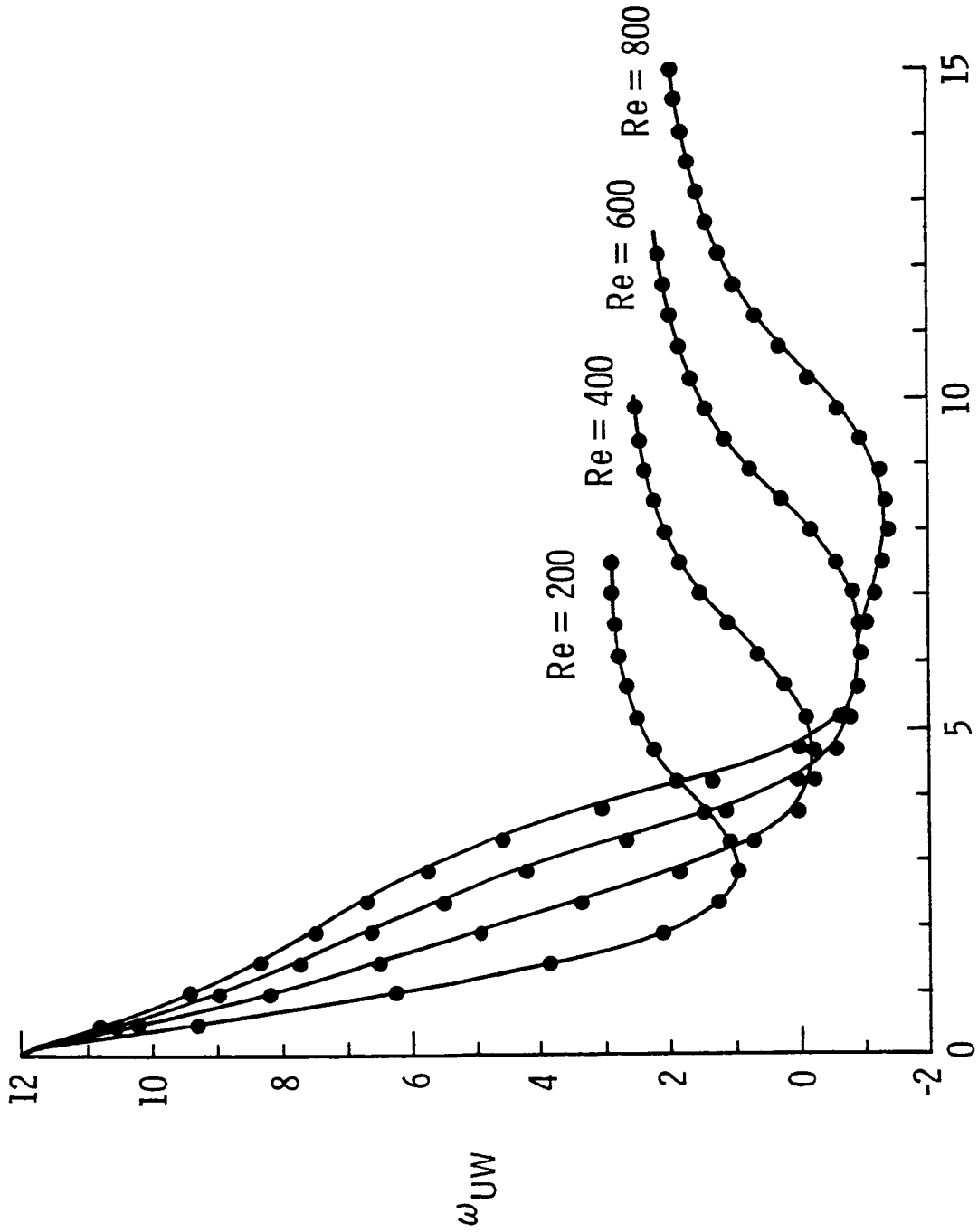

Figure 12

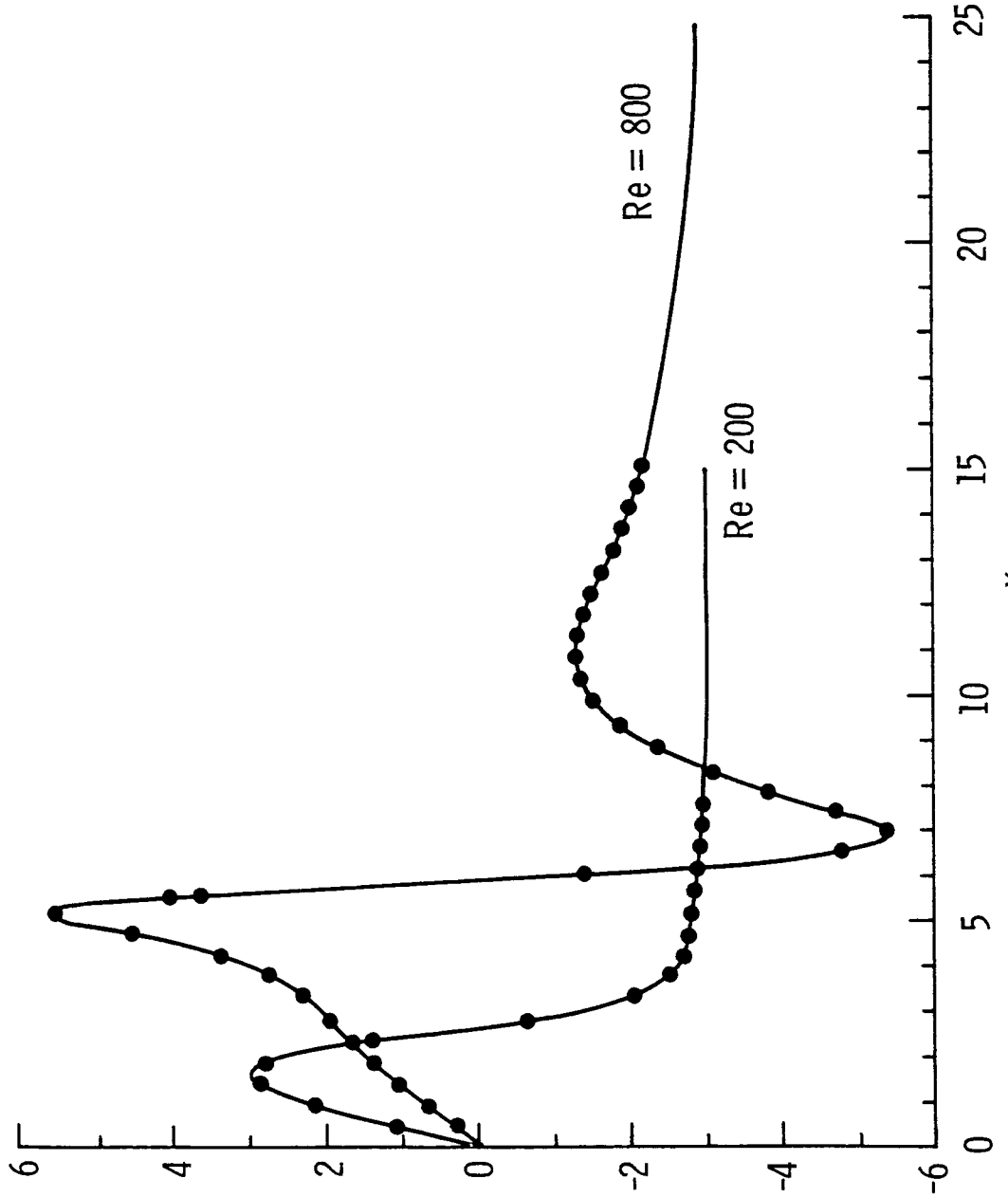

Figure 13

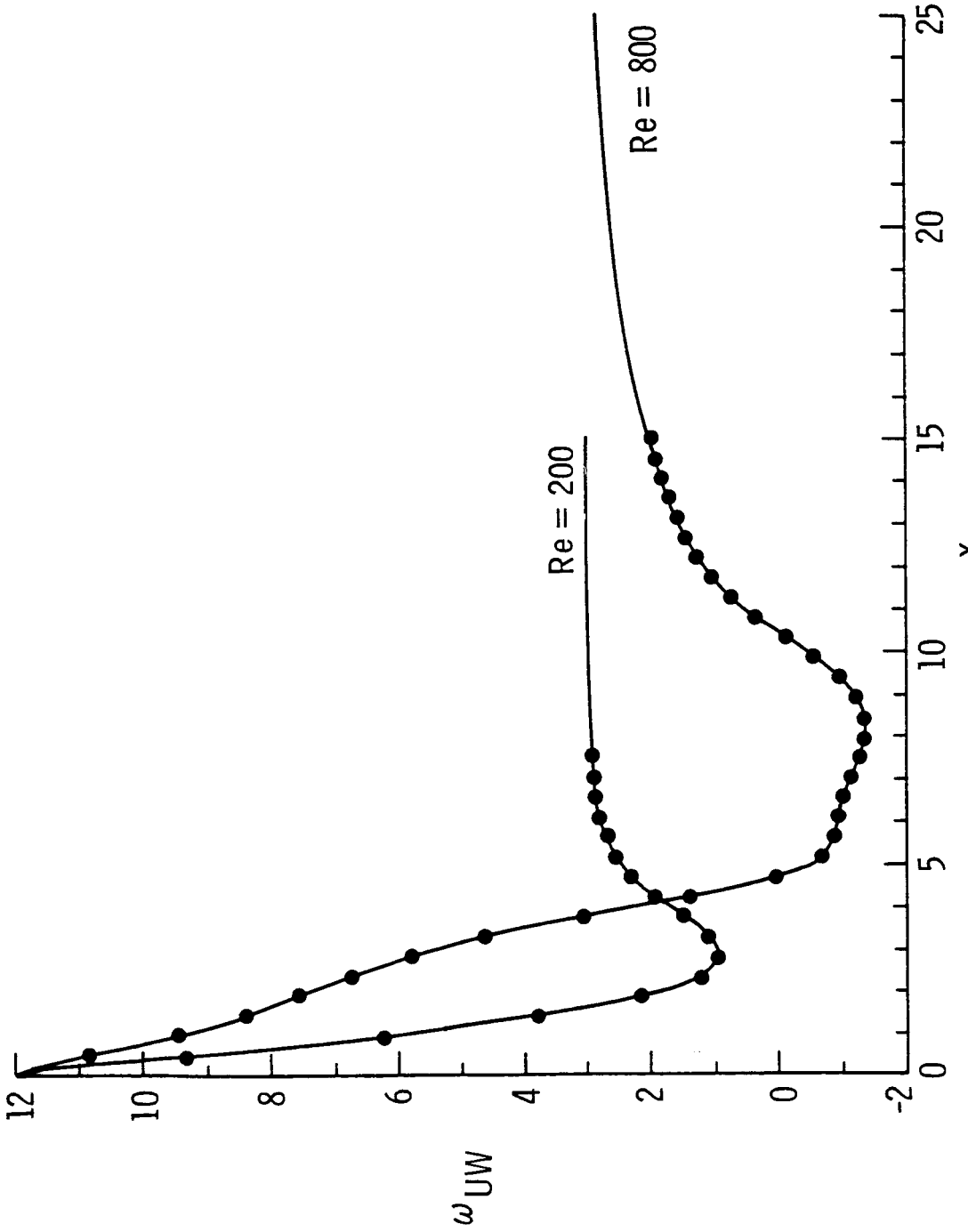

Figure 14

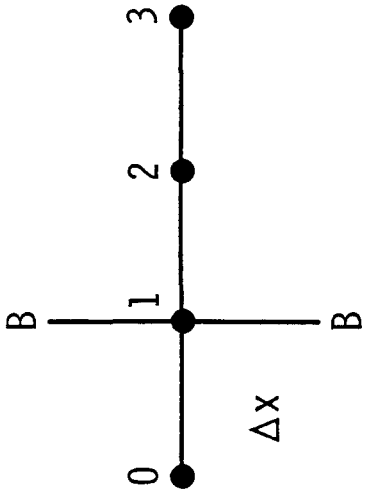

Figure 15

Standard Bibliographic Page

1. Report No. NASA CR-178197 ICASE Report No. 86-68	2. Government Accession No.	3. Recipient's Catalog No.
4. Title and Subtitle EFFICIENT SOLUTIONS OF TWO-DIMENSIONAL INCOMPRESSIBLE STEADY VISCOUS FLOWS		5. Report Date October 1986 6. Performing Organization Code
7. Author(s) J. H. Morrison, M. Napolitano		8. Performing Organization Report No. 86-68
9. Performing Organization Name and Address Institute for Computer Applications in Science and Engineering Mail Stop 132C, NASA Langley Research Center Hampton, VA 23665-5225		10. Work Unit No. 11. Contract or Grant No. NAS1-18107
12. Sponsoring Agency Name and Address National Aeronautics and Space Administration Washington, D.C. 20546		13. Type of Report and Period Covered Contractor Report 14. Sponsoring Agency Code 505-90-21-01

15. Supplementary Notes

Langley Technical Monitor:
J. C. South

Final Report

Submitted to Computers and Fluids

16. Abstract

This paper provides a simple, efficient, and robust numerical technique for solving two-dimensional incompressible steady viscous flows at moderate-to-high Reynolds numbers. The proposed approach employs an incremental multigrid method and an extrapolation procedure based on minimum residual concepts to accelerate the convergence rate of a robust block-line-Gauss-Seidel solver for the vorticity-stream function Navier-Stokes equations.

Results are presented for the driven cavity flow problem using uniform and nonuniform grids and for the flow past a backward facing step in a channel. For this second problem, mesh refinement and Richardson extrapolation are used to obtain useful benchmark solutions in the full range of Reynolds numbers at which steady laminar flow is established.

17. Key Words (Suggested by Authors(s))	18. Distribution Statement
Navier-Stokes, multigrid	34 - Fluid Mechanics and Heat Transfer 64 - Numerical Analysis Unclassified - unlimited

19. Security Classif.(of this report)	20. Security Classif.(of this page)	21. No. of Pages	22. Price
Unclassified	Unclassified	44	A03

For sale by the National Technical Information Service, Springfield, Virginia 22161